Radiocarbon, Vol 66, Nr 6, 2024, p 1869–1882 DOI:10.1017/RDC.2024.8
Selected Papers from the 24th Radiocarbon and 10th Radiocarbon & Archaeology International Conferences, Zurich, Switzerland, 11–16 Sept. 2022

CARBON ISOTOPE CHANGES THROUGH THE RECENT PAST: $F^{14}C$ AND $\delta^{13}C$ VALUES IN SINGLE BARLEY GRAIN FROM 1852 TO 2020

E Dunbar[1]* • E M Scott[2] • B G Tripney[1]

[1]Scottish Universities Environmental Research Centre, Scottish Enterprise Technology Park, East Kilbride, Glasgow, G75 0QF, Scotland, UK
[2]School of Mathematics and Statistics, University of Glasgow, Glasgow G12 8QQ, Scotland, UK

ABSTRACT. Radiocarbon ($F^{14}C$) and stable carbon ($\delta^{13}C$) values were measured in single grains of spring barley (*Hordeum vulgare L.*) from the sample archive from two adjacent sites of the Long-term Experiments (LTEs) Hoosfield Spring Barley at Rothamsted Research (Harpenden, Hertfordshire, UK), covering the growing periods (March to September) of 1852 to 2020. $F^{14}C$ data of the barley grain confirm that recent values are approaching and will decline below the "nominal" $F^{14}C$ value of 1, tracking a similar decrease reported in other studies. Importantly, the measured $\delta^{13}C$ values reveal a different temporal decline over the pre-bomb and post-bomb timescale. Detailed statistical analysis of $\delta^{13}C$ data along with $\delta^{13}C$ analysis of independent, archived barley mash samples, verifies and quantifies the extent and rate of this decline. Evidence presented from the barley grain and barley mash samples suggests a clear breakpoint in $\delta^{13}C$ data occurring in 1995, where the rate of change alters, in that the slope in $\delta^{13}C$ data for the pre-1995 period is declining at 1.4‰ per century, and the slope in $\delta^{13}C$ for the post-1995 period is declining at 3.6‰ per century. Such a consistent shift in $\delta^{13}C$ data could be used with $F^{14}C$ values to extend the use of the bomb peak for forensic, ecological, and environmental applications.

KEYWORDS: barley grain, bomb curve, $F^{14}C$ values, temporal $\delta^{13}C$.

INTRODUCTION AND BACKGROUND

The ^{14}C released by nuclear weapons tests during the 1950s and early 1960s indirectly created a diagnostic "bomb curve" of enhanced ^{14}C levels in the environment. This rapid increase in ^{14}C values, and subsequent decrease via the uptake of $^{14}CO_2$ by the biosphere and oceans, can be used to determine the age of short-lived materials for forensic applications, and offers insight into changes within the global carbon cycle. In the same timeframe, increasing greenhouse gas (GHG) emissions from fossil fuel burning continued to alter the $^{13}CO_2$ and $^{12}CO_2$ content in the atmosphere, with a resulting relative dilution of the ^{14}C content. Both these anthropogenic episodes influence the natural atmospheric ^{14}C activity ("fraction modern" $F^{14}C$) and $\delta^{13}C$ values, as first predicted by Suess in the 1950s (Suess 1953).

The natural $F^{14}C$ value is nominally set at a value of 1, almost reaching a value of 2 in 1963 when the nuclear weapons test ban treaty came into action and is presently approaching the "nominal" $F^{14}C$ value of 1 due to uptake by the biosphere and ocean, and increased fossil fuel emissions. While the widespread decline in $F^{14}C$ values below 1 will make the use of the diagnostic bomb curve problematic in the next few years, estimates of the rate and extent of decline below 1 are variable (Sierra 2018).

The fluctuations in atmospheric ^{14}C concentrations and ancillary $\delta^{13}C$ values have been monitored for many decades through direct atmospheric monitoring of CO_2 (Levin and

*Corresponding author. Email: elaine.dunbar@glasgow.ac.uk

Hesshaimer 2000; Manning et al. 1990; Nydal and Lövseth 1996; Hua et al. 2013; Hua et al. 2022), or using annual $F^{14}C$ records, with studies based on measurements of single tree rings (Reimer et al. 2013, 2020), grain with a single, known year of growth (Hüls et al. 2021) or wines and spirits to infer atmospheric $F^{14}C$ levels (Baxter 1969; PhD thesis).

Additional studies have confirmed an increase in CO_2 concentration and a temporal shift in $\delta^{13}C$ values in atmospheric measurements over the industrial period, monitored and identified in the Scripps CO_2 Program since the late 1950s (https://scrippsco2.ucsd.edu/). $\delta^{13}C$ measurements on air extracted from Antarctic ice core sections also confirm recent increasing CO_2 concentration and a decline in $\delta^{13}C$ (Etheridge et al. 1996; Francey et al. 1999). The compiled records of carbon isotopes in atmospheric CO_2 produced by Graven et al. (2017) reveal evidence of temporal changes in $\delta^{13}C$ within the atmosphere.

$F^{14}C$ and $\delta^{13}C$ data obtained from tree-ring studies have confirmed a decline in $\delta^{13}C$ values observed over the industrial period (Freyer 1979; Stuiver et al. 1998; McCarroll et al. 2009; Graven et al. 2017; Reimer et al. 2020) only partly explained by changes in the isotopic ratio of CO_2, and correction procedures have been derived to estimate $\delta^{13}C$ values that would have been obtained under pre-industrial conditions (McCarroll et al. 2009).

Radiocarbon analysis of local annual plants has been used to infer atmospheric radiocarbon concentration in cities globally, providing an estimate of CO_2 data during a growing season (Sierra 2018; Hüls et al. 2021). Single year grain samples have been studied at SUERC for many years, forming part of the routine Quality Assurance procedures used in the SUERC Radiocarbon Laboratory. Many of these single year grain samples have also been used in International Radiocarbon Intercomparison studies over the past 30 years and reliable consensus values for the $F^{14}C$, and data for $\delta^{13}C$, are available (Baxter 1990; Scott et al. 2007; Scott et al. 2010a; Scott et al. 2010b; Scott et al. 2016). The evaluation of our internal quality assurance data collected over many years indicated there was a potential change in $\delta^{13}C$ values with time. Additional analysis of single year derived ethanol confirmed that there was a drift in $\delta^{13}C$ values with time (Dunbar et al. 2018, Cook et al. 2020). Conveniently, these observed changes in $\delta^{13}C$ values in the late 20th century can be used to help identify which side of the diagnostic radiocarbon bomb curve (Hua et al. 2022) a sample may derive from i.e., the upslope or the downslope (Dunbar et al. 2018; Cook et al. 2020).

Presented in this paper are radiocarbon $F^{14}C$ and $\delta^{13}C$ values of duplicate grain samples from two adjacent sites deriving from 1852 until 2020. The new barley grain data are presented together with data from archive barley mash samples, some of which formed part of the International Radiocarbon Intercomparison studies over the past 30 years. This detailed dataset will be used to monitor $F^{14}C$ levels and determine whether a temporal trend in $\delta^{13}C$ values exists within one geographical area. The additional $F^{14}C$ measurements from these barley grain samples add to the $F^{14}C$ data available over the pre-and post-bomb timeline, while detailed statistical analysis of the $\delta^{13}C$ values will verify and quantify if any temporal shift in $\delta^{13}C$ exists. As $F^{14}C$ values approach and decline below 1 it will be problematic to establish if biological materials are pre- or post-bomb. However, if there is a measurable shift in $\delta^{13}C$ values within environmental compartments, e.g., biota, as $F^{14}C$ decline below 1, this shift in $\delta^{13}C$ can be used in conjunction with the measured $F^{14}C$ values to extend the use of the bomb peak. Here the question asked is, if $\delta^{13}C$ values of a single crop species were measured over a large time frame can we estimate the change in $\delta^{13}C$ values occurring from the same geographical location, with a restricted land use?

https://doi.org/10.1017/RDC.2024.8 Published online by Cambridge University Press

METHODS

Biota of known date and provenance, beginning in the pre-nuclear era, are ideal for observing changing $F^{14}C$ and $\delta^{13}C$ values within a single geographical region over the last 100-150 years. Rothamsted Research (Hertfordshire, UK) is home to the oldest continuing agricultural field experiments in the world, and is located 35 km north of London, UK (Latitude 51° 48' 34.44" N; Longitude 0° 21' 22.76" W), covering about 330 ha. Seven of these Long-Term Experiments (LTEs) continue today, including the Hoosfield Spring Barley which is an archive of annual grain samples from different agricultural experiments dating back to 1852. Permission was granted by Rothamsted Research to obtain archived spring barley grain samples from every 2–3 years between 1852–2020. Paired samples of barley grain grown in the same year were taken from two different treatment plots with a relatively constant history of fertiliser or manure inputs.

The bulk barley mash samples are archived Quality Assurance materials regularly measured in the SUERC laboratory. This processed barley mash material was obtained from various distilleries across Scotland and provides an ideal, independently sourced material for comparison, although the precise geographical origin of the barley is unknown.

SAMPLING

Barley (*Hordeum vulgare L.*) is a member of the grass family and is a major cereal grain cultivated in the UK, with an average spring growing season from March to September. Annual records from the "Yields of the Long-Term Experiments" are available on the electronic Rothamsted Documents Archive: e-RAdoc (https://www.era.rothamsted.ac.uk/eradoc/books/2) and confirm that the spring barley was sown in late March and harvested in late August/early September (± 1–2 weeks). The Hoosfield Spring Barley grain samples were grown in two different treatment plots, Plot 72 (FYMN0 – plot 72) and Plot 42 (N1PK-plot-42). Both plots have a constant history of fertiliser or manure inputs and are located within 20m of each other. The plots are similar in soil composition and drainage, and are subject to comparable environmental factors, such as rainfall, temperature, prevailing wind direction, and other atmospheric considerations.

The barley grain was harvested, dried, and stored in sealed glass bottles since their year of collection. For this study, 2-3 grains were selected from each plot from the year specified. In total 112 barley grain samples were sampled from the archive. The years of crop and barley varieties are detailed in Table 1.

Sample Pretreatment

Each grain was acid rinsed for 1–2 seconds with 0.1M HCl to remove residual grain and soil detritus, rinsed with deionised water, and dried overnight at 40°C (Dunbar et al. 2016). The barley grain remained intact. Half a single grain (each grain was halved down the centre midline, typically 20–30 mg) was weighed into a clean quartz insert for combustion (Vandeputte et al. 1996). The barley mash samples were acid rinsed with 0.1M HCl, rinsed with deionised water, and dried overnight at 40°C. Typically, 15 mg of barley mash was weighed into a clean quartz insert for combustion (Vandeputte et al. 1996). Replicate quality assurance standards generated from combustion of a single year of barley mash from the Glengoyne distillery, Sample A in the Third International Radiocarbon Intercomparison (TIRI) (Naysmith et al. 2010) were also prepared. The resulting CO_2 was cryogenically isolated

https://doi.org/10.1017/RDC.2024.8 Published online by Cambridge University Press

Table 1 Rothamsted Long-term Experiment: Hoosfield Spring barley varieties 1852–2021.

Year of crop	Hoosfield; spring barley variety
1852–80	Chevalier
1881–90	Archer's Stiff Straw
1891–97	Carter's Paris Prize
1898–01	Archer's Stiff Straw
1902–05	Hallet's Pedigree Chevalier
1906–16	Archer's Stiff Straw
1917–63	Plumage Archer (Spratt Archer 1927, 1929–32)
1964–66	Plumage Archer and Maris Badger compared
1968–69	Maris Badger
1970–79	Julia
1980–83	Georgie
1984–91	Triumph
1992–95	Alexis
1996–99	Cooper
2000–7	Optic
2008–2015	Tipple
2016–present	Irina

Notes: fallowed in 1912, 1933, 1943 and 1967 to control weeds. Short–strawed cultivars introduced in 1970.

Table 2 $F^{14}C$ for TIRI A and $\delta^{13}C$ for Quality Assurance Samples used at SUERC RCL.

	Consensus $F^{14}C$ value (± 1σ)	SUERC $F^{14}C$ value (± 1σ)	SUERC mean $\delta^{13}C$ value (± 1σ)
Barley Mash TIRI sample A	1.1635 ± 0.0085	1.1660 ± 0.0024 (n = 8)	–26.3 ± 0.3 (n = 8)
Kerosene	n/a	0.0016 ± 0.0004 (n = 11)	–30.5 ± 0.3 (n = 11)
Anthracite	n/a	0.0016 ± 0.0004 (n = 11)	–23.3 ± 0.3 (n = 11)
Distilled ethanol (2006)	n/a	1.0615 ± 0.0043 (n = 11)	–27.8 ± 0.2 (n = 11)

and 3 mL subsamples were converted to graphite using the zinc and iron reduction method described by Slota et al. (1987).

Radiocarbon Analysis

The $F^{14}C$ measurements were undertaken using a National Electrostatics Corporation (NEC) 5MV tandem accelerator mass spectrometer using a 134-position MC-SNICS source for running samples (Dunbar et al. 2016). Supplemental quality assurance standards were included in the measurement batch and the data listed in Table 2. The measured $F^{14}C$ values for the Rothamsted archive barley grain for Plot 72 and Plot 42 are listed in Table 3.

https://doi.org/10.1017/RDC.2024.8 Published online by Cambridge University Press

Table 3 Rothamsted Long-term Experiment: Hoosfield Spring barley varieties $F^{14}C$ and $\delta^{13}C$ values, 1852–2020.

Year	Date sown	Date of harvest	Lab code	Plot 72 $F^{14}C$ value	Error ± 1σ	Plot 72 $\delta^{13}C$	Error ±1σ	Lab code	Plot 42 $F^{14}C$ value	Error	Plot 42 $\delta^{13}C$	Error ± 1σ	$F^{14}C$ value from calibration curve data*	Standard deviation $F^{14}C$
1852	05/03/1852	24/08/1852	SUERC-104674	0.9785	0.0029	–24.0	0.1	SUERC-104808	0.9866	0.0021	–25.1	0.1	0.9844	0.0012
1855	29/03/1855	24/08/1855	SUERC-104675	0.9852	0.0029	–25.4	0.1	SUERC-104809	0.9890	0.0029	–25.7	0.1	0.9843	0.0012
1858	20/03/1858	04/08/1858	SUERC-104676	0.9822	0.0029	–24.9	0.1	SUERC-104810	0.9876	0.0029	–24.3	0.1	0.9846	0.0012
1861	No date	20/08/1861	SUERC-104677	0.9808	0.0029	–25.6	0.1	SUERC-104811	0.9875	0.0029	–25.9	0.1	0.9844	0.0012
1864	26/03/1864	11/08/1864	SUERC-104678	0.9837	0.0029	–23.5	0.1	SUERC-104812	0.9797	0.0029	–24.2	0.1	0.9841	0.0012
1867	05/04/1867	20/08/1867	SUERC-104679	0.9893	0.0026	–23.7	0.1	SUERC-104813	0.9908	0.0029	–25.0	0.1	0.9846	0.0012
1870	15/03/1870	27/07/1870	SUERC-104683	0.9833	0.0029	–24.5	0.1	SUERC-104817	0.9825	0.0029	–22.4	0.1	0.9847	0.0012
1873	28/03/1873	20/08/1873	SUERC-104684	0.9832	0.0025	–23.8	0.1	SUERC-104818	0.9823	0.0023	–25.3	0.1	0.9841	0.0011
1876	23/03/1876	07/08/1876	SUERC-104685	0.9803	0.0029	–24.1	0.1	SUERC-104819	0.9778	0.0025	–24.7	0.1	0.9839	0.0011
1879	10/03/1879	01/09/1879	SUERC-104686	0.9850	0.0025	–25.7	0.1	SUERC-104820	0.9845	0.0029	–25.3	0.1	0.9851	0.0011
1882	11/03/1882	17/08/1882	SUERC-104687	0.9832	0.0025	–24.8	0.1	SUERC-104821	0.9925	0.0029	–25.1	0.1	0.9859	0.0011
1885	12/03/1885	14/08/1885	SUERC-104688	0.9796	0.0029	–24.2	0.1	SUERC-104822	0.9861	0.0029	–23.4	0.1	0.9857	0.0011
1888	05/04/1888	08/09/1888	SUERC-104689	0.9837	0.0023	–25.1	0.1	SUERC-104823	0.9912	0.0029	–25.3	0.1	0.9858	0.0012
1891	23/02/1891	31/08/1891	SUERC-104694	0.9870	0.0029	–24.7	0.1	SUERC-104828	0.9858	0.0029	–25.5	0.1	0.9868	0.0012
1894	07/03/1894	15/08/1894	SUERC-104695	0.9877	0.0021	–24.6	0.1	SUERC-104829	0.9883	0.0029	–25.4	0.1	0.9878	0.0012
1897	23/03/1897	18/08/1897	SUERC-104696	0.9820	0.0029	–24.1	0.1	SUERC-104830	0.9891	0.0029	–24.5	0.1	0.9878	0.0011
1900	12/03/1900	16/08/1900	SUERC-104697	0.9809	0.0029	–24.4	0.1	SUERC-104831	0.9874	0.0026	–22.6	0.1	0.9881	0.0011
1903	21/02/1903	02/09/1903	SUERC-104698	0.9868	0.0023	–25.1	0.1	SUERC-104832	0.9790	0.0029	–25.4	0.1	0.9881	0.0011
1906	19/03/1906	20/08/1906	SUERC-104699	0.9856	0.0029	–24.1	0.1	SUERC-104833	0.9830	0.0029	–24.1	0.1	0.9869	0.0012
1909	06/04/1909	08/09/1909	SUERC-104703	0.9865	0.0029	–24.8	0.1	SUERC-104837	0.9806	0.0029	–25.9	0.1	0.9857	0.0012
1913	06/03/1913	21/08/1913	SUERC-104704	0.9806	0.0029	–24.1	0.1	SUERC-104838	0.9850	0.0029	–25.2	0.1	0.9852	0.0012
1916	04/04/1916	01/09/1916	SUERC-104705	0.9801	0.0029	–24.0	0.1	SUERC-104839	0.9812	0.0029	*–25.9*	0.1	0.9844	0.0012
1919	08/04/1919	09/09/1919	SUERC-104706	0.9829	0.0029	–25.1	0.1	SUERC-104840	0.9831	0.0029	–25.9	0.1	0.9833	0.0012
1923	20/04/1923	22/08/1923	SUERC-104707	0.9818	0.0029	–24.1	0.1	SUERC-104841	0.9710	0.0023	–24.5	0.1	0.9824	0.0012
1926	08/04/1926	25/08/1926	SUERC-104708	0.9745	0.0025	–25.5	0.1	SUERC-104842	0.9876	0.0029	–25.4	0.1	0.9811	0.0012
1929	17/04/1929	28/08/1929	SUERC-104709	0.9811	0.0029	–23.3	0.1	SUERC-104843	0.9715	0.0029	–24.1	0.1	0.9800	0.0012
1932	09/03/1932	23/08/1932	SUERC-104714	0.9772	0.0029	–24.2	0.1	SUERC-104848	0.9626	0.0025	–25.5	0.1	0.9799	0.0012
1935	08/03/1935	14/08/1935	SUERC-104715	0.9719	0.0029	–25.3	0.1	SUERC-104849	0.9691	0.0029	–25.9	0.1	0.9803	0.0012
1938	25/02/1938	04/08/1938	SUERC-104716	0.9704	0.0029	–25.8	0.1	SUERC-104850	0.9704	0.0029	–24.7	0.1	0.9799	0.0012
1941	17/03/1941	22/08/1941	SUERC-104717	0.9705	0.0023	–26.1	0.1	SUERC-104851	0.9660	0.0029	–25.1	0.1	0.9790	0.0003
1944	29/03/1944	18/08/1944	SUERC-104718	0.9661	0.0029	–24.7	0.1	SUERC-104852	0.9654	0.0021	–23.6	0.1	0.9786	0.0001
1947	17/04/1947	18/08/1947	SUERC-104719	0.9679	0.0029	–25.3	0.1	SUERC-104853	0.9586	0.0028	–25.7	0.1	0.9780	0.0001
1950	24/03/1950	14/08/1950	SUERC-104723	0.9654	0.0029	–25.5	0.1	SUERC-104857	0.9679	0.0021	–25.9	0.1	0.9740	0.0002
1954	07/04/1954	16/09/1954	SUERC-104724	0.9772	0.0029	–25.4	0.1	SUERC-104858	0.9752	0.0029	–25.6	0.1	0.9892	0.0024
1957	06/05/1957	29/08/1957	SUERC-104725	1.0830	0.0025	–26.0	0.1	SUERC-104859	1.0873	0.0028	–25.1	0.1	1.0755	0.0063
1960	07/04/1960	05/09/1960	SUERC-104726	1.2325	0.0036	*–24.7*	0.1	SUERC-104860	1.2405	0.0036	–25.5	0.1	1.2170	0.0189

(Continued)

Table 3 (*Continued*)

Year	Date sown	Date of harvest	Lab code	Plot 72 $F^{14}C$ value	Error ± 1σ	Plot 72 $\delta^{13}C$	Error ±1σ	Lab code	Plot 42 $F^{14}C$ value	Error	Plot 42 $\delta^{13}C$	Error ± 1σ	$F^{14}C$ value from calibration curve data*	Standard deviation $F^{14}C$
1963	24/04/1963	17/09/1963	SUERC-104727	1.9126	0.0056	–25.1	0.1	SUERC-104861	1.9258	0.0057	–25.1	0.1	1.6566	0.1845
1966	18/03/1966	26/08/1966	SUERC-104728	1.7252	0.0050	–24.4	0.1	SUERC-104862	1.7076	0.005	–26.2	0.1	1.7021	0.0088
1968	04/03/1968	22/08/1968	SUERC-104729	1.6040	0.0047	–25.6	0.1	SUERC-104863	1.5849	0.0047	–25.5	0.1	1.5875	0.0166
1971	24/02/1971	11/08/1971	SUERC-104734	1.5192	0.0045	–25.7	0.1	SUERC-104868	1.5337	0.0039	–25.9	0.1	1.5180	0.0197
1974	26/03/1974	31/08/1974	SUERC-104735	1.4453	0.0037	–25.7	0.1	SUERC-104869	1.4410	0.0037	–24.9	0.1	1.4209	0.0033
1977	08/03/1977	23/08/1977	SUERC-104736	1.3611	0.0040	–25.5	0.1	SUERC-104870	1.3592	0.0035	–25.7	0.1	1.3392	0.0041
1980	21/02/1980	18/08/1980	SUERC-104737	1.2894	0.0028	–25.3	0.1	SUERC-104871	1.2944	0.0033	–26.6	0.1	1.2728	0.0032
1983	09/03/1983	09/08/1983	SUERC-104738	1.2540	0.0037	–24.6	0.1	SUERC-104872	1.2606	0.0037	–25.8	0.1	1.2347	0.0025
1986	17/03/1986	29/08/1986	SUERC-104739	1.2006	0.0028	–25.2	0.1	SUERC-104873	1.1950	0.0035	–25.1	0.1	1.1936	0.0031
1989	07/02/1989	01/08/1989	SUERC-104743	1.1568	0.0034	–25.4	0.1	SUERC-104877	1.1647	0.0030	–24.6	0.1	1.1703	0.0020
1992	26/02/1992	05/08/1992	SUERC-104744	1.1289	0.0033	–25.3	0.1	SUERC-104878	1.1379	0.0030	–26.7	0.1	1.1393	0.0029
1995	16/03/1995	08/08/1995	SUERC-104745	1.1236	0.0026	–26.1	0.1	SUERC-104879	1.1203	0.0029	–25.6	0.1	1.1194	0.0014
1999	12/02/1999	24/08/1999	SUERC-104746	1.1024	0.0032	–26.0	0.1	SUERC-104880	1.0961	0.0032	–26.4	0.1	1.0970	0.0017
2001	30/03/2001	06/09/2001	SUERC-104747	1.0930	0.0032	–26.5	0.1	SUERC-104881	1.0938	0.0028	–26.5	0.1	1.0861	0.0027
2004	12/02/2004	06/08/2004	SUERC-104748	1.0753	0.0032	–27.3	0.1	SUERC-104882	1.0707	0.0028	–26.5	0.1	1.0691	0.0022
2007	02/02/2007	03/09/2007	SUERC-104749	1.0656	0.0032	–26.7	0.1	SUERC-104883	1.0602	0.0031	–28.2	0.1	1.0579	0.0011
2010	11/03/2010	31/08/2010	SUERC-104754	1.0515	0.0031	–26.9	0.1	SUERC-104888	1.0551	0.0031	–28.7	0.1	1.0476	0.0005
2013	01/03/2013	27/08/2013	SUERC-104755	1.0355	0.0027	–26.9	0.1	SUERC-104889	1.0296	0.0031	–26.7	0.1	1.0301	0.0026
2016	29/02/2016	24/08/2016	SUERC-104756	1.0236	0.0030	–28.5	0.1	SUERC-104890	1.0291	0.0030	–28.0	0.1	1.0195	0.0014
2020	24/03/2020	01/09/2020	SUERC-104757	1.0065	0.0024	–25.9	0.1	SUERC-104891	1.0118	0.0024	–26.4	0.1		

*$F^{14}C$ value 1852–1938 IntCal20, Reimer et al. (2020), 1941–2020 (average for March to September calculated), Bomb21NH1, Hua et al. (2022).

Table 4 Glasgow International Radiocarbon Intercomparison Studies barley mash sample $F^{14}C$ consensus values and SUERC RCL measured $\delta^{13}C$ values.

International Radiocarbon Intercomparison Study ID (year of collection)	Barley Mash $F^{14}C$ consensus value	Error ± 1σ	SUERC measured $\delta^{13}C$ (n = variable)
TIRI A (1991)	116.35	0.0085	–26.5 (n = 2)
FIRI G (1998)	110.70	0.04	–28.8 (n = 2)
VIRI A (2001)	109.10	0.04	–28.6 (n = 2)
SIRI D (2006)	103.90	0.0630	–30.4 (n = 5)
GIRI A (1991)	116.52 SUERC $F^{14}C$	0.6	–26.5 (n = 1)
GIRI C (2017)	102.25 SUERC $F^{14}C$	0.43	–30.5 (n = 3)
GIRI F (2019)	101.56 SUERC $F^{14}C$	0.43	–28.5 (n = 4)

Stable Isotope Measurements

$\delta^{13}C$ analyses were performed on subsamples of CO_2 using a VG SIRA II IRMS. Sample values are compared with those of working standard reference gases of known isotopic composition, produced from international reference materials NBS19 and IAEA-CO-1. The measurement results are expressed using the δ notation (Craig 1957) as per mil deviations from the VPDB standard, with 1σ precision of ±0.1‰. CO_2 aliquots from the primary and secondary ^{14}C standards were also measured (oxalic acid II primary standard, humic acid secondary standard, and a barley mash or a background secondary standard) detailed in Dunbar et al. (2016). These values are used for offline normalization of sample $^{14}C/^{13}C$ ratios. Supplementary $\delta^{13}C$ values for anthracite and kerosine standards, used in the SUERC RCL, were measured to establish mean $\delta^{13}C$ values for comparison (Table 2). The measured $\delta^{13}C$ values for the Rothamsted archive barley grain and barley mash data are listed in Table 3 and Table 4, respectively.

Statistical Models

For the investigation of the temporal trend, a dog-leg (or changepoint) linear regression model was developed. This model (either with known or unknown changepoint) was compared using ANOVA to a simple, single linear regression (Julious 2001). The model is defined in the equations below.

$$\delta^{13}C_i = f(t_i) = \alpha_1 + \beta_1 t_i \text{ for } t_0 \le t_i \le d$$

$$\delta^{13}C_i = f(t_i) = \alpha_2 + \beta_2 t_i \text{ for } d \le t_i \le t_1$$

and subject to $\alpha_1 + \beta_1 d = \alpha_2 + \beta_2 d$

where d is the changepoint, and t is year.

RESULTS AND DISCUSSION

$F^{14}C$

Presented in Table 3 are the radiocarbon $F^{14}C$ and $\delta^{13}C$ values in duplicate grain samples from two adjacent sites at Rothamsted, deriving from 1852 until 2020. The annual growing seasons for the barley grain samples are detailed in Table 3 and range from March through to

https://doi.org/10.1017/RDC.2024.8 Published online by Cambridge University Press

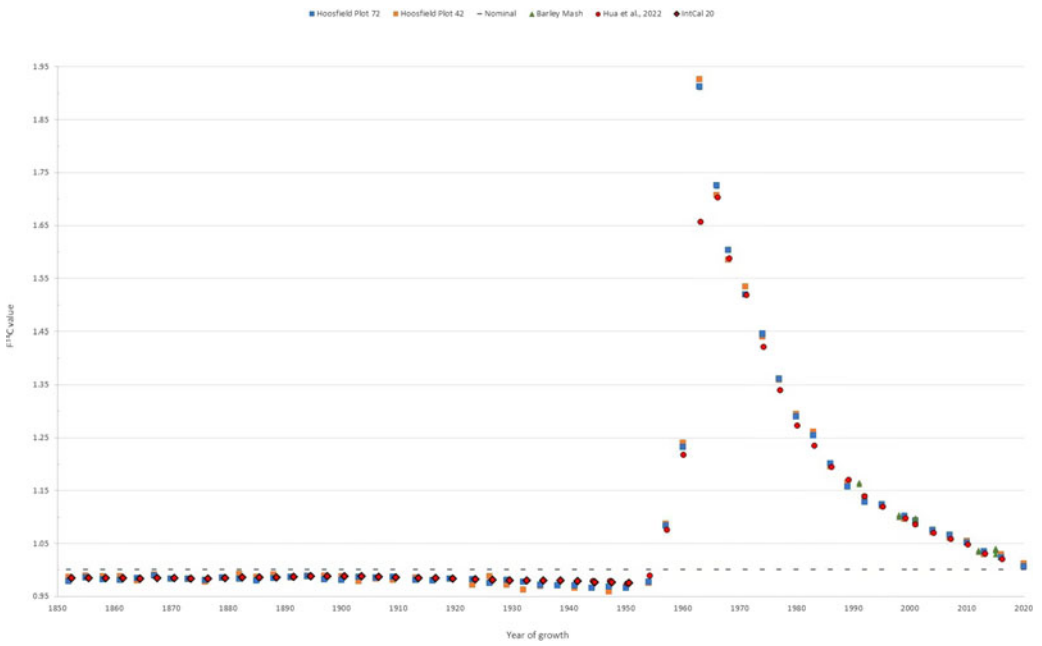

Figure 1 $F^{14}C$ values for barley grain samples at Rothamsted Long-term Experiment: Hoosfield Spring barley varieties 1852–2020 and Barley Mash (data from IntCal20, Reimer et al. 2020 [red diamond] and Hua et al. 2022 [red circle] are shown alongside). (Please see online version for color figures.)

September (https://www.era.rothamsted.ac.uk/eradoc/books/2). Also included, for comparison in Table 3 are $F^{14}C$ values, for 1852 to 1938 from IntCal20 (Reimer et al. 2020) and for 1941 to 2020 (average March to September data estimated) from Northern Hemisphere Zone 1 data (Hua et al. 2022).

The CO_2 generated and graphitised from each grain sample is representative of carbon assimilated within the plant in this growth season timeframe. The uptake of carbon and growth of the grain throughout a season is highly complex, with many processes from photosynthesis, carbon accumulation, and subsequent redistribution of carbon within the cereal. For comparison of the yearly data presented here, it is assumed that carbon assimilation occurs within a similar time frame each year.

Comparing the $F^{14}C$ values from the barley grain at Rothamsted sites Plot 72 and Plot 42, presented in Figure 1 and Table 3, with the $F^{14}C$ values for the pre-bomb timeline 1852 to 1940 from the IntCal20 calibration curve (Reimer et al. 2020), suggests there is good general agreement between the Rothamsted barley grain data and the measured atmospheric $F^{14}C$ data sets. $F^{14}C$ values of barley grain from both Rothamsted plots reached their lowest values of 0.9654 ± 0.0029 in 1950, and 0.9586 ± 0.0029 in 1947, respectively, both are slightly lower than the estimated average for the NH Zone 1 for the period to September. These slightly lower values observed at Rothamsted in 1947 and 1950 may be the result of a few local or regional factors, possibly due to additional coal burning in the immediate post war period. The steady decline of $F^{14}C$ values immediately prior to the onset of nuclear weapons testing corresponds with the observed continuous decline of atmospheric $\delta^{13}C$ data on a global scale, detailed in Table 3 and shown in Figure 1.

https://doi.org/10.1017/RDC.2024.8 Published online by Cambridge University Press

The barley grain $F^{14}C$ values from 1941 to 2016, spanning the bomb peak period, were compared with the estimated average $F^{14}C$ values for the growing season (average for March to September) from NH Zone 1 data, as listed in Table 3 (Hua et al. 2022). From Figure 1, the data between the paired barley grain begins to deviate in 1960, but notably higher $F^{14}C$ values of 1.9126 ± 0.0056 and 1.9258 ± 0.0057 are identified in the barley grains from both Rothamsted plots in 1963, compared with a growing season estimate of $F^{14}C$ 1.6566 ± 0.1845 from the NH Zone 1 atmospheric data. Figure 1 illustrates that Rothamsted grain $F^{14}C$ data is consistently higher than the global average measured in following years, 1966 until 1983, suggesting that the influence of enhanced $^{14}CO_2$ derived from the weapons testing was observed in the Rothamsted area, reaching higher ^{14}C levels faster, and remaining elevated for longer. It must be considered that variation exists around the NH Zone 1 data, and local influences are a contributing factor. In the years since 1983 the Rothamsted data remain slightly higher than the atmospheric NH Zone 1 data. The most recent year sampled with grain and NH Zone 1 data for comparison is 2016, with Rothamsted data remaining slightly higher than the NH Zone 1 value, with paired values of 1.0236 ± 0.003 and 1.0291 ± 0.0003 compared with the average for March to September $F^{14}C$ value of 1.0195 ± 0.0014 (Hua et al. 2022). Recent grain harvested in 2020 had measured $F^{14}C$ values of 1.0065 ± 0.0024 from Plot 72 and 1.0118 ± 0.0024 from Plot 42, both approaching the "nominal" $F^{14}C$ value of 1 (Figure 1), however no additional data was available for comparison.

Additionally, the supplemental barley mash $F^{14}C$ data from the Intercomparison study samples collected over the last 30 years (Table 4) have decreased at a similar rate to the atmospheric levels (Hua et al. 2022) and the paired barley grain, with recent $F^{14}C$ levels remaining slightly above the "nominal" value of 1. It should be noted however that the barley mash differs from barley grain in that it is a processed material with the carbohydrate and protein fractions removed, i.e., the mash material is largely residual "husk". The geographical location where the source barley was grown is confidential, so little comment can be made concerning the local $^{14}CO_2$.

$\delta^{13}C$

The $\delta^{13}C$ values for the barley grain plotted in Figure 2 suggest that, before 1960, values are relatively constant with a mean $\delta^{13}C = -22.3 \pm 1.2‰$, with a shift to an average value of $-26.8 \pm 0.98‰$ post-2000. The $\delta^{13}C$ values start decreasing in both plots in the early 2000s (Figure 2). It must be noted that a small systematic offset of 0.268 ± 0.12‰ is observed between the annual paired $\delta^{13}C$ measurements on the barley grain from each site. This offset between Plot 72 and Plot 42 remains unexplained as the sites are <20m apart and have undergone similar treatments within the timescale.

The original TIRI-A barley mash sample was collected in 1990 and has a mean $\delta^{13}C$ value of –26.5‰ (n = 10), decreasing to –30.6‰ (n = 20), in the 2015 sample. A shift in $\delta^{13}C$ values is also evident in the Barley Mash data from the replicate measurements (Table 4, Figure 2).

A basic linear regression (purple curve) with a segmented (dog-leg) regression (blue curve) fitted to the measured $\delta^{13}C$ data (Figure 3) shows that there is a clear breakpoint at 1995, when the rate of change in $\delta^{13}C$ has a negative slope, pre-1995, of 1.4‰ per century, and similarly, a negative slope, post-1995, of 3.6‰ per century. Measurement of "corrected" $\delta^{13}C$ values from tree ring data obtained from different sites in Northern Europe spanning the 19th and 20th centuries by McCarroll et al. (2009) show variation in $\delta^{13}C$ decline, as do the compiled studies

https://doi.org/10.1017/RDC.2024.8 Published online by Cambridge University Press

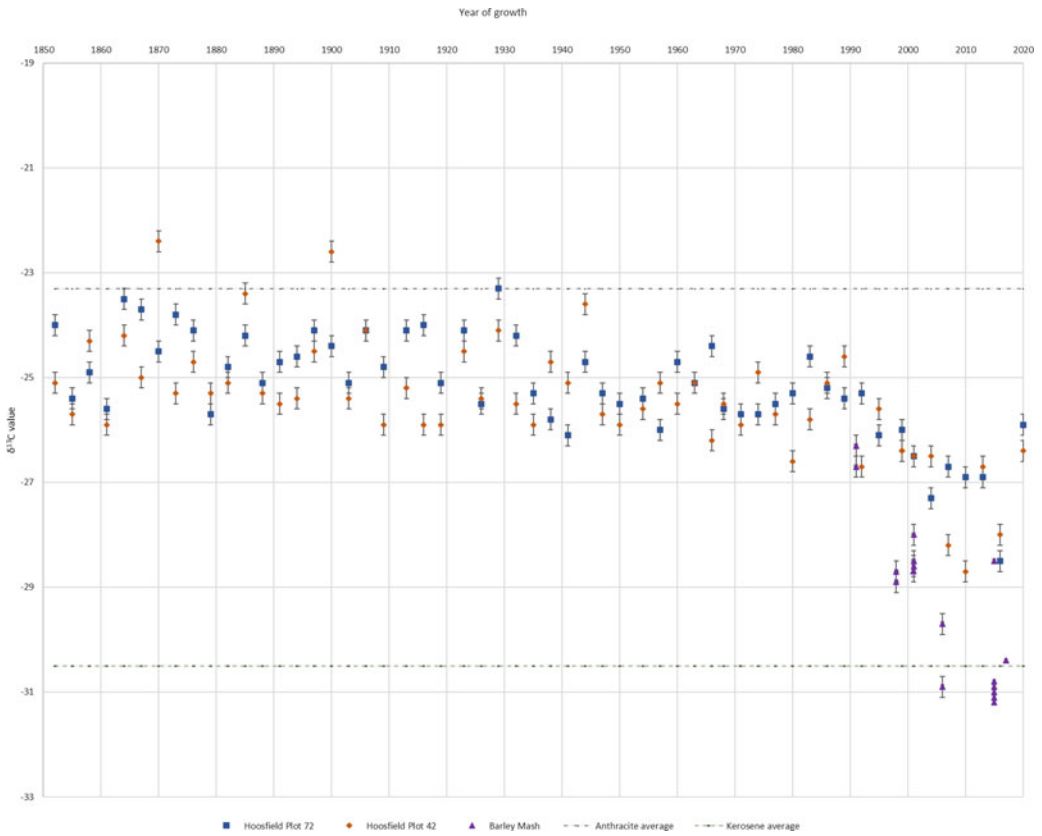

Figure 2 $\delta^{13}C$ values for barley grain samples at Rothamsted Long-term Experiment: Hoosfield Spring barley varieties 1852–2020.

from different location and sample types by Graven et al. (2017). These studies highlight that the rate of decline varies with sample type, location and the timeline applied. The reasons for this apparent change in $\delta^{13}C$ pre- and post-1995 at this location remains highly complex and additional data is required. Although Rothamsted Research is the location of a weather station; CO_2 data are not available over the timeline investigated. As a result, no corrections were applied to the $\delta^{13}C$ values of the barley grain to account for any temporal trend in atmospheric $\delta^{13}CO_2$ values—the appropriate correction is being considered.

Ongoing investigations include considering whether there are local sources of fossil carbon. According to recent data (Ritchie et al. 2023), CO_2 emissions from UK fossil fuel sources have been declining since 1995.

DISCUSSION

The global carbon cycle is made more complex in the industrial period by the introduction of human sources interacting with natural atmospheric CO_2 processes. There are many other external factors that influence the $\delta^{13}CO_2$ but the most significant to be considered in the recent industrial period is the use of petroleum and natural gas. Studies simulating the $F^{14}C$ bomb peak levels, with and without the effect of fossil fuels, have shown the potential impact of fossil

https://doi.org/10.1017/RDC.2024.8 Published online by Cambridge University Press

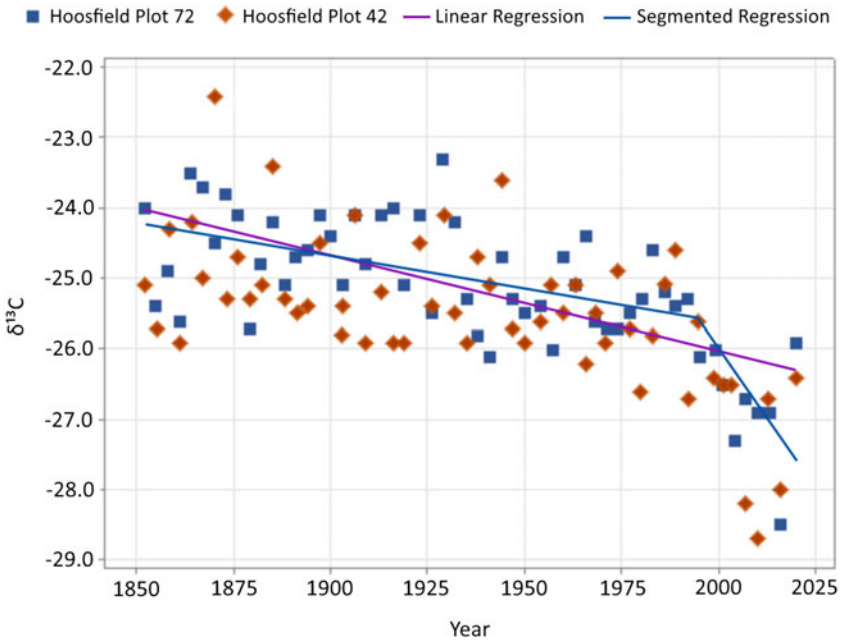

Figure 3 Linear and Segmented Regression of $\delta^{13}C$ values for barley grain samples at Rothamsted Long-term Experiment: Hoosfield Spring barley varieties 1852–2020.

fuels on CO_2 concentration and composition (Graven et al. 2020). The average $\delta^{13}C$ value of anthracite is –23.3‰ (n = 11) whereas petroleum-based kerosine is –30.5‰ (n = 11) (Table 2 and Figure 2). While the $\delta^{13}C$ of natural gas is source dependant, a $\delta^{13}C$ value of –44.2‰ has been identified in the natural gas fuel supply of an urban area (Pugliese et al. 2017). Although anthracite burning has been common in the UK since the industrial revolution, the use of petroleum and natural gas has significantly increased in the last few decades. To some extent the impact of the use of anthracite will not be overly apparent in the $\delta^{13}C$ value of the barley grain samples, as the values are too similar to those observed in archaeological barley grain with an average $\delta^{13}C$ of –23.8‰ (n = 100). As Figure 2 illustrates, petroleum-based products have a distinctly different $\delta^{13}C$ value. There are many factors that might influence $\delta^{13}CO_2$, however using both $F^{14}C$ and $\delta^{13}C$ measurements together may permit triangulation and identification of organic materials of recent origin. Anomalous $\delta^{13}C$ values of –25.9‰ and –26.4‰ were observed for both Plot 72 and Plot 42 in 2020 inconsistent with the observed trend. The obvious assumption is an association with the temporary alteration in daily CO_2 emissions during the COVID-19 compulsory confinement. Barley grains for 2021 and 2022 were not available at the time of analysis. Establishing the $\delta^{13}C$ and $F^{14}C$ values from barley grain grown annually since 2020 will determine if this $\delta^{13}C$ re-bound is indeed an anomaly, and if $\delta^{13}C$ values will again continue to demonstrate more negative values.

CONCLUSIONS

This paper presents $F^{14}C$ and $\delta^{13}C$ values in paired barley grain samples from 1852 to 2020 in one geographical location, using archive material from Rothamsted Research. The $F^{14}C$ values of barley grain and bulk barley mash intercomparison samples show a similar trend to the values from Reimer et al. (2020) and Hua et al. (2022), demonstrating that $F^{14}C$ values at the

https://doi.org/10.1017/RDC.2024.8 Published online by Cambridge University Press

Rothamsted site unsurprisingly follow the global atmospheric trend, but are offset in that the paired barley grain from Rothamsted $F^{14}C$ levels increase at a faster rate, and remain high over a longer period. Analysis of the $\delta^{13}C$ measurements from the barley grain and bulk barley mash samples reveal a temporal shift with statistical analysis suggesting a clear breakpoint occurring in 1995 where the rate of change in $\delta^{13}C$ alters, in that $\delta^{13}C$, pre-1995, is declining at 1.4‰ per century, while $\delta^{13}C$, post-1995, is declining at 3.6‰ per century. The reason for this shift in the rate of decline is complex, but it is noted that the values are becoming more similar to those from petroleum and natural gas resources, the use of which continues to increase globally, but many external causes could be influential.

The $F^{14}C$ values of the barley grain samples will decline below the nominal $F^{14}C$ value of 1 within 2–3 years, however the quantifiable shift in $\delta^{13}C$ values within the last 30 years presents a potentially useful indicator to identify pre- and post-bomb peak $F^{14}C$ data. Further analysis and data are required to establish if this trend is replicated in other C3 and C4 biota, for example $\delta^{13}C$ values may be readily available from other temporal studies of similar plant materials, making it possible that widespread $\delta^{13}C$ alterations could be used with the $F^{14}C$ values to extend the use of the bomb peak for forensic, ecological, and environmental applications.

ACKNOWLEDGMENTS

Rothamsted Research is a world-leading, non-profit research centre that focuses on strategic agricultural science to the benefit of farmers and society worldwide. Rothamsted Research is the longest-running agricultural research institution in the world. The authors would like to thank Dr Andy MacDonald and Holly Addis for their assistance gaining permission to obtain the samples from the archive, and for their help during the sampling process and Dr Andy Gregory for comments.

We thank the Lawes Agricultural Trust and Rothamsted Research for data from the e-RA database. The Rothamsted Long-term Experiments National Bioscience Research Infrastructure (RLTE-NBRI) is supported by the UK BBSRC (Biotechnology and Biological Sciences Research Council, BBS/E/C/000J0300, 2017-2023) and the Lawes Agricultural Trust. We are grateful to the referees for their constructive input reviewing the manuscript.

REFERENCES

Baxter MS. 1969. Recent fluctuations of Atmospheric ^{14}Carbon Concentrations [PhD thesis]. The University of Glasgow Radiocarbon Laboratory (SUERC).

Baxter MS. 1990. International Workshop of Intercomparison of Radiocarbon Laboratories: welcome – the aims – the programme. Radiocarbon 32:253–255.

Craig H. 1957. Isotopic standards for carbon and oxygen and correction factors for mass-spectrometric analysis of carbon dioxide. Geochemica et Cosmochimica Acta 12(1–2): 133–149.

Cook GT, Dunbar E, Tripney BG, Fabel D. 2020. Using carbon isotopes to fight the rise in fraudulent whisky. Radiocarbon 62:51–62.

Dunbar E, Cook GT, Naysmith P, Tripney B, Xu S. 2016. AMS ^{14}C dating at the Scottish Universities Environmental Research Centre (SUERC) Radiocarbon Dating Laboratory. Radiocarbon 58:9–23.

Dunbar E, Cook G, Murdoch I, Xu S, Fabel D. 2018. Identification of fraudulent-age whiskies using accelerator mass spectrometry (AMS) radiocarbon (^{14}C) analyses. In: Proceedings of the Worldwide Distilled Spirits Conference 2017.

Etheridge DM, Steele LP, Langenfelds RL, Francey RJ, Barnola JM, Morgan VI. 1996. Natural and anthropogenic changes in atmospheric CO_2 over the last 1000 years from air in Antarctic ice and firn. J. Geophys. Res. 101(D2):4115–4128.

https://doi.org/10.1017/RDC.2024.8 Published online by Cambridge University Press

Francey RJ, Allison CE, Etheridge DM, Trudinger CM, Enting IG, Leuenberger M, Langenfelds RL, Michel E, Steele LP. 1999. A 1000-year high precision record of $\delta^{13}C$ in atmospheric CO_2, Tellus B: Chemical and Physical Meteorology 51(2):170–193.

Freyer HD. 1979. On the ^{13}C record in tree rings. Part I. ^{13}C Variations in northern hemispheric trees during the last 150 years. Tellus 31:124–137.

Graven H, Allison CE, Etheridge DM, Hammer S, Keeling RF, Levin I, Meijer HAJ, Rubino M, Tans PP, Trudinger CM, Vaughn BH, White JWC. 2017. Compiled records of carbon isotopes in atmospheric CO_2 for historical simulations in CMIP6. Geoscientific Model Development 10:4405–4417.

Graven H, Keeling RF, Rogelj J. 2020. Changes to carbon isotopes in atmospheric CO_2 over the industrial era and into the future. Global Biogeochemical Cycles: an International Journal of Global Change 34:1–21.

Hua Q, Barbetti M, Rakowski AZ. 2013. Atmospheric Radiocarbon for the Period 1950–2010. Radiocarbon 55:2059–2072.

Hua Q, Turnbull J, Santos G, Rakowski A, Ancapichún S, De Pol-Holz, R, Turney C. 2022. Atmospheric radiocarbon for the period 1950–2019. Radiocarbon 64:723–745.

Hüls CM, Börner A, Hamann C. 2021. Wheat seed (*Triticum Aestivum* L.) Radiocarbon concentration over the last 75 years. Radiocarbon 63:1387–1396.

Julious S. 2001. Inference and estimation in a changepoint regression problem. The Statistician 50(1):51–61.

Levin I, Hesshaimer V. 2000. Radiocarbon—a unique tracer of global carbon cycle dynamics. Radiocarbon 42:69–80.

Manning M, Lowe D, Melhuish, W, Sparks R, Wallace G, Brenninkmeijer C, McGill R. 1990. The use of radiocarbon measurements in atmospheric Studies. Radiocarbon 32:37–58.

McCarroll D, Gagen M, Loader N, Robertson I, Anchukaitis K, Los S, Young G, Jalkanen R, Kirchhefer A, Waterhouse J. 2009. Correction of tree ring stable carbon isotope chronologies for changes in the carbon dioxide content of the atmosphere. Geochimica et Cosmochimica Acta 73:1539–1547.

Naysmith P, Cook GT, Freeman SPHT, Scott EM, Anderson R, Xu S, Dunbar E, Muir GKP, Dougans A, Wilcken K, Schnabel C, Russell N, Ascough PL, Maden C. 2010. ^{14}C AMS at SUERC: Improving QA data with the 5 MV tandem AMS and 250 kV SSAMS. Radiocarbon 52:263–271.

Nydal R and Lövseth K. 1996. Carbon-14 measurement in atmospheric CO_2 from Northern and Southern Hemisphere sites, 1962–1993. Oak Ridge, Tennessee, USA: Carbon Dioxide Information Analysis Center–World Data Center–A for Atmospheric Trace Gases.

Pugliese SC, Murphy JG, Vogel F, Worthy D. 2017. Characterization of the $\delta^{13}C$ signatures of anthropogenic CO_2 emissions in the Greater Toronto Area, Canada. Applied Geochemistry 83:171–180.

Reimer PJ, Bard E, Bayliss A, Beck JW, Blackwell PG, Bronk Ramsey C, Buck C, Cheng H, Edwards RL, Friedrich M, et al. 2013. IntCal13 and Marine13 radiocarbon age calibration curves 0–50,000 years cal BP. Radiocarbon 55(4):1869–1887. doi: 10.2458/azu_js_rc.55.16947

Reimer PJ, Austin WEN, Bard E, Bayliss A, Blackwell PG, Ramsey CB, Butzin M, Cheng H, Edwards RL, Friedrich M, et al. 2020. The IntCal20 Northern Hemisphere radiocarbon age calibration curve (0–55 cal kBP). Radiocarbon 62(4):725–757. doi: 10.1017/RDC.2020.41

Ritchie H, Rosado P, Roser M. 2023. CO_2 and Greenhouse Gas Emissions. Published online at OurWorldInData.org. Retrieved from: https://ourworldindata.org/co2-and-greenhouse-gas-emissions [Online Resource].

Rothamsted Research. 2023. Yields of the Long-Term Experiments. Available on the electronic Rothamsted Documents Archive: e-RAdoc (https://www.era.rothamsted.ac.uk/eradoc/books/2) [Online Resource]

Scott EM, Cook GT, Naysmith P, Bryant C, O'Donnell D. 2007. A report on phase 1 of the 5th International Radiocarbon Intercomparison (VIRI). Radiocarbon 49:409–426.

Scott EM, Cook GT, Naysmith P. 2010a. A report on phase 2 of the Fifth International Radiocarbon Intercomparison (VIRI). Radiocarbon 52: 846–858.

Scott EM, Cook GT, Naysmith P. 2010b. The Fifth International Radiocarbon Intercomparison (VIRI): an assessment of laboratory performance in stage 3. Radiocarbon 52: 859–865.

Scott EM, Naysmith P, Cook GT. 2016. A report on the Sixth International Radiocarbon Intercomparison (SIRI). Radiocarbon 59: 1589–1596.

Sierra CA. 2018. Forecasting atmospheric radiocarbon decline to pre-bomb values. Radiocarbon 60:1055–1066.

Slota PJ Jr, Jull AJT, Linick TW, Toolin LJ. 1987. Preparation of small samples for ^{14}C accelerator targets by catalytic reduction of CO. Radiocarbon 29:303–306.

Stuiver M, Reimer P, Braziunas T. 1998. High-precision radiocarbon age calibration for terrestrial and marine samples. Radiocarbon 40(3):1127–1151.

Suess HE. 1953. Natural radiocarbon and the rate of exchange of carbon dioxide between the

https://doi.org/10.1017/RDC.2024.8 Published online by Cambridge University Press

atmosphere and the sea. In: Nuclear Processes in Geological Settings. National Research Council Publications 52–56.

UC San Diego, Scripps Institution of Oceanography. The Keeling Curve. Scripps CO_2 Program, (https://scrippsco2.ucsd.edu/). [Online Resource]

Vandeputte K, Moens L, Dams R. 1996. Improved sealed-tube combustion of organic samples to CO_2 for stable carbon isotope analysis, radiocarbon dating and percent carbon determinations. Analytical Letters 29: 2761–2773.

https://doi.org/10.1017/RDC.2024.8 Published online by Cambridge University Press